

## Fabrication and characterization of an AlGa<sub>N</sub>/PZT detector\*

Zhang Yan(张燕)<sup>1,†</sup>, Sun Jinglan(孙璟兰)<sup>2</sup>, Wang Nili(王妮丽)<sup>1</sup>, Han Li(韩莉)<sup>2</sup>,  
Liu Xiangyang(刘向阳)<sup>1</sup>, Li Xiangyang(李向阳)<sup>1</sup>,  
and Meng Xiangjian(孟祥建)<sup>2</sup>

(1 State Key Laboratory of Transducer Technology, Shanghai Institute of Technical Physics, Chinese Academy of Sciences, Shanghai 200083, China)

(2 National Laboratory for Infrared Physics, Shanghai Institute of Technical Physics, Chinese Academy of Sciences, Shanghai 200083, China)

**Abstract:** Design, fabrication and characterization of a novel two-color detector for ultraviolet and infrared applications are reported. The detector has a simple multilayer structure composed of n-Al<sub>0.3</sub>Ga<sub>0.7</sub>N/i-GaN/p-GaN/SiO<sub>2</sub>/LaNiO<sub>3</sub>/PZT/Pt fabricated on a sapphire substrate. Ultraviolet and infrared properties are measured. For the ultraviolet region, a flat band spectral response is achieved in the 302–363 nm band. The detector displays an unbiased responsivity of 0.064 A/W at 355 nm. The current–voltage curve shows that current at zero bias is  $-1.57 \times 10^{-12}$  A. This led to a detectivity of  $1.81 \times 10^{11}$  cm · Hz<sup>1/2</sup>/W. In the infrared region, the detectivity of the detector is  $1.58 \times 10^5$  cm · Hz<sup>1/2</sup>/W at 4 μm.

**Key words:** AlGa<sub>N</sub>/PZT; dual-band detector; UV/IR; responsivity; detectivity

**DOI:** 10.1088/1674-4926/31/12/124015 **EEACC:** 2520

### 1. Introduction

In the past few years, the development in imaging system applications has led to an interest in detectors with two or three different wavelength responses<sup>[1,2]</sup>. For example, the missile named ‘stringer post’ with CdS/InSb detectors can detect objects with both ultraviolet and infrared radiation, and it performed very well in the Afghanistan war<sup>[3]</sup>. However, research into dual-band detectors is mostly focused on the infrared range. In 2005, an MWIR/LWIR HgCdTe FPA with a scale of 640 × 480 was reported. For other wavelengths, developments are far behind the demand. In this paper, a new type of UV/IR detector with an AlGa<sub>N</sub>/PZT structure is designed and fabricated. The performances of the detector are measured.

### 2. Fabrication of devices

In order to detect light with different wavelengths simultaneously, two active areas are designed in perpendicular geometry. The detector has a simple multilayer structure composed of n-Al<sub>0.3</sub>Ga<sub>0.7</sub>N/i-GaN/p-GaN/SiO<sub>2</sub>/LaNiO<sub>3</sub>/PZT/Pt fabricated on a sapphire substrate. A schematic cross section is shown in Fig. 1. Light illuminates from the backside. The ultraviolet photons and the infrared photons are absorbed by different layers.

A double-side-polished sapphire was selected as the substrate to allow the incident radiation from the backside of the detector. On top of this, an AlN buffer layer was deposited by low-pressure metal organic chemical vapor deposition<sup>[4]</sup>. The n-type lateral conduction layer consisting of Al<sub>0.3</sub>Ga<sub>0.7</sub>N:Si was grown at an intermediate temperature. The carrier concentration was expected to exceed  $1 \times 10^{18}$  cm<sup>-3</sup>. The active region for the ultraviolet radiation consisted of a sim-

ple p–i–n junction with a 150 nm-thick GaN intrinsic region and a 150 nm-thick p-GaN layer. A 200 nm-thick SiO<sub>2</sub> passivation layer and then a 500 nm thick aerogel SiO<sub>2</sub> thermal isolation layer were deposited on the AlGa<sub>N</sub> multilayer subsequently<sup>[5]</sup>. LaNiO<sub>3</sub> and PZT were grown by a sol–gel method, and the former acted as both electrode and absorbing layer. Pt was then evaporated at the top of the PZT as the upper electrode. The electrode contact windows to the underlying layers—n-AlGa<sub>N</sub>, p-GaN and LaNiO<sub>3</sub>—were formed using ionized beam etching. In/Au metals were then evaporated onto the n-AlGa<sub>N</sub> layer, and Ni/Au to both the p-GaN and the LaNiO<sub>3</sub> layer, using an electron-beam evaporator. In this way, a two-color detector with three electrode terminals was achieved. A top view of the detector is shown in Fig. 2.

### 3. Electrical and optical properties of the device

*I–V* measurement of the p-GaN/i-GaN/n-AlGa<sub>N</sub> junction of the detector was carried out with a KEITHLEY236. This

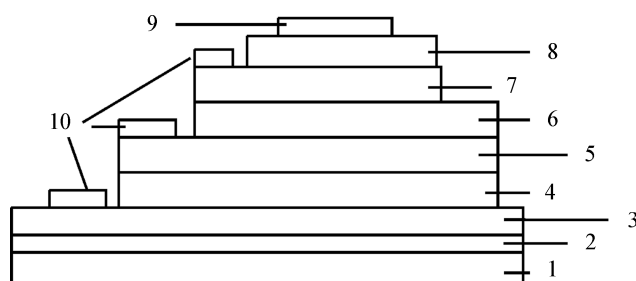


Fig. 1. Structure of back-illuminated AlGa<sub>N</sub>/PZT detector. 1: Sapphire substrate; 2: AlN buffer layer; 3: n-AlGa<sub>N</sub>; 4: i-GaN; 5: p-GaN; 6: SiO<sub>2</sub>; 7: LaNiO<sub>3</sub>; 8: PZT; 9: Pt; 10: Au.

\* Project supported by the National Natural Science Foundation of China (No. 60807037).

† Corresponding author. Email: zhangyan@mail.sitp.ac.cn

Received 7 June 2010, revised manuscript received 12 August 2010

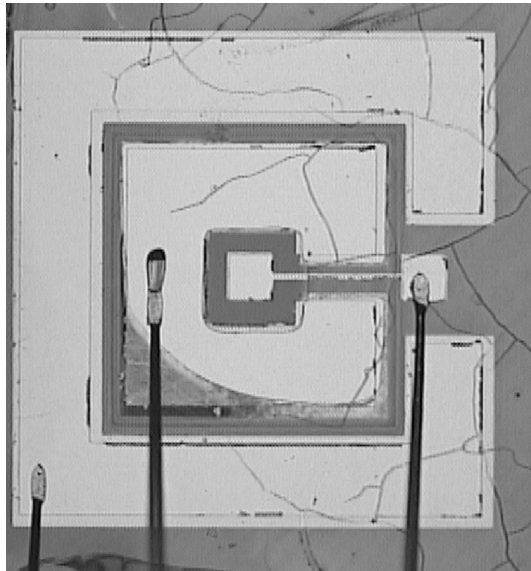


Fig. 2. Top view of the detector.

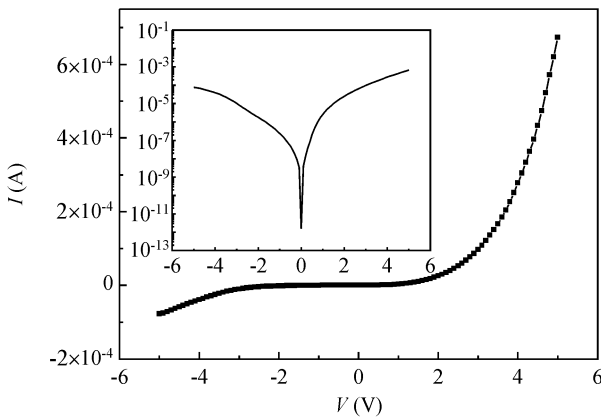
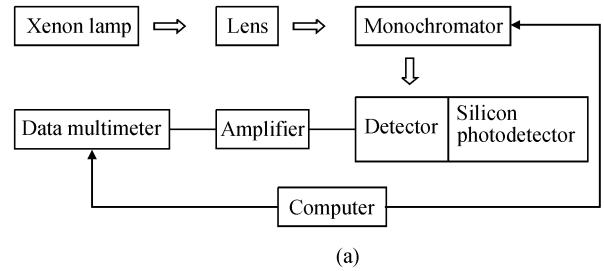


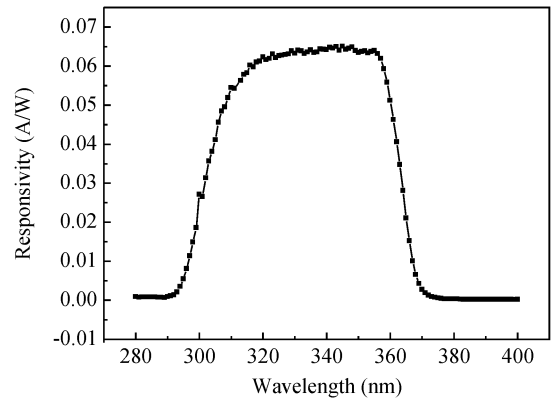
Fig. 3.  $I-V$  curve of the ultraviolet-region shown in linear scale. The inset shows the same data in logarithmic scale.

$I-V$  curve has a typical diode feature (shown in Fig. 3). The current at zero voltage bias was  $-1.57 \times 10^{-12}$  A. The dynamic resistance at zero voltage was  $2.71 \times 10^7 \Omega$ , thus  $R_0A = 4.44 \times 10^5 \Omega \cdot \text{cm}^2$  was obtained. A large leakage current density as high as  $4.74 \times 10^{-3} \text{ A/cm}^2$  was found at  $-5$  V. This may be related to the cracks on the surface of the samples (as can be seen in Fig. 2). These cracks appeared after the deposition of PZT thin film on the top of the  $\text{SiO}_2$  layer. The surface morphology of the PZT layer can be transferred to the ultraviolet active region during the etching process. Damage to this active region causes degradation in the ultraviolet performance of the detector<sup>[6]</sup>.

The photoresponse of the detector to ultraviolet radiation was measured using a high intensity xenon lamp with 350 W power, calibrated with a UV-enhanced silicon photodetector. Light current produced from the detector was magnified by a Stanford SR570 amplifier and then collected by a VC98 data multimeter. The measurement equipment and the photoresponse under back illumination are shown in Fig. 4. A flat band spectral response was observed in the UV wavelength range from 302 to 363 nm. The inter-band absorption in n-AlGaIn



(a)



(b)

Fig. 4. (a) Measurement equipment. (b) Optical responsivity of detector in the ultraviolet region.

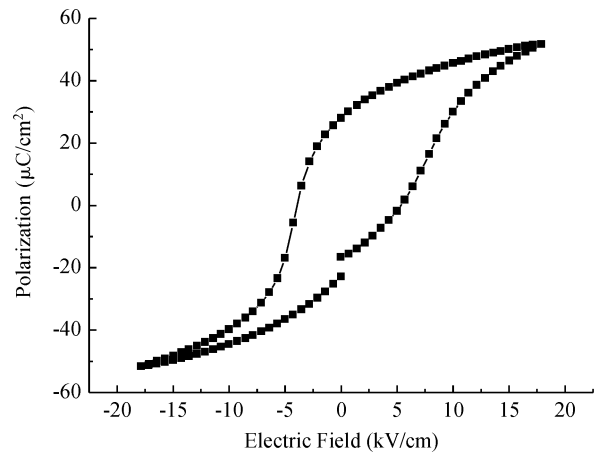


Fig. 5. Hysteresis loop of the LNO/PZT/Pt capacitor.

produced the sharp short-wavelength cutoff at 302 nm. The detector showed an unbiased responsivity of 0.064 A/W at 355 nm, which corresponds to a value of 22.4% for the external quantum efficiency of the device. Considering the loss from sapphire absorption and interface reflection of about 15%, the  $\eta$  is estimated to be 26.3%. Combining with  $R_\lambda = 0.064 \text{ A/W}$ ,  $A = 4.1 \times 10^{-3} \text{ cm}^2$ , we achieved a detectivity performance of  $D_\lambda^* = 1.81 \times 10^{11} \text{ cm} \cdot \text{Hz}^{1/2}/\text{W}$  at  $\lambda = 355 \text{ nm}$ . A hysteresis loop of an LNO/PZT/Pt ferroelectric capacitor is shown in Fig. 5. The optical response is measured using a standard system. The light from a blackbody is modulated before being received by this novel detector. The detectivity of the device is  $1.58 \times 10^5 \text{ cm} \cdot \text{Hz}^{1/2}/\text{W}$  with the blackbody temperature set at 773 K and the chopper frequency at 7 Hz for the infrared part. This result is related to the cracks on the surface of the sam-

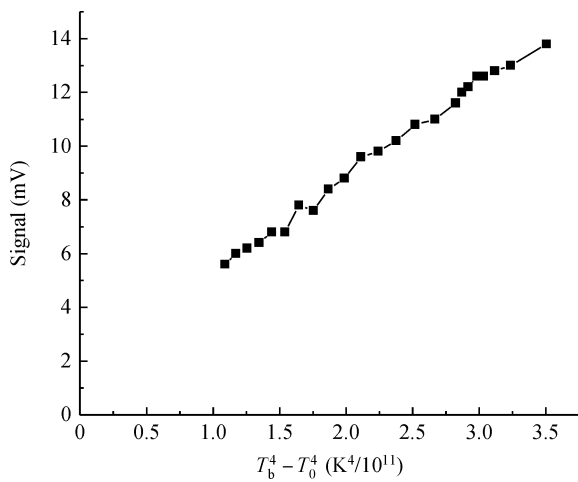


Fig. 6. IR signal changing with blackbody temperature.

ples to some degree. The response of the detector versus the blackbody temperature was measured. The voltage response of the detector against  $T_b^4 - T_0^4$  is plotted in Fig. 6. The straight line indicates that LNO is a good absorbing layer with a uniform absorption of the incident infrared radiation with different wavelengths.

In summary, the AlGaIn/PZT detectors with a multilayer structure composed of n-Al<sub>0.3</sub>Ga<sub>0.7</sub>N/i-GaN/p-

GaN/SiO<sub>2</sub>/LaNiO<sub>3</sub>/PZT/Pt can operate in both the ultraviolet and the infrared regions. For the ultraviolet region, the response spectrum is 302–363 nm and the responsivity value at 355 nm is 0.064 A/W. For the infrared region, it displayed the detectivity performance of  $1.58 \times 10^5 \text{ cm} \cdot \text{Hz}^{1/2}/\text{W}$ . Because of surface cracks, the performance is not as good as we expected. We will focus on the crack generation and try to fabricate a crack-free detector in further research.

## References

- [1] Rogalski A. Dual-band infrared detectors. *Proc SPIE*, 2000, 3948: 17
- [2] Antoni R. Third-generation infrared photon detectors. *Opt Eng*, 2003, 42(12): 3498
- [3] Shen Junping, Liu Jianyong, Hu Jianghua, et al. Study on a integrative countermeasure of armed helicopter to counter IR/UV dual colour guidance. *Infrared Technol*, 2005, 27(6): 505 (in Chinese)
- [4] Zhou Zhongtang, Guo Liwei, Xing Zhigang, et al. Growth of semi-insulating GaN by using two-step AlN buffer layer. *Chin Phys Lett*, 2007, 24(6): 1641
- [5] Fricke J, Emmerling A. Aerogels-recent progress in production detector techniques and novel applications. *Journal of Sol-Gel Science and Technology*, 1998, 13: 299
- [6] Chen Jie, Xu Jintong, Wang Ling, et al. Low-damage wet chemical etching for GaN-based visible-blind p-i-n detector. *Proc SPIE*, 2008, 6621: 66211D